Array Architecture for Wideband Transmit Nulling

Peter G. Vouras and Jean W. de Graaf
The Naval Research Laboratory
Washington, DC 20375

***Abstract*— The ability to create nulls in the transmit pattern of a phased array antenna has many applications for communication and radar systems, including interference and clutter mitigation. Most nulling techniques introduce small perturbations in amplitude and phase, or phase-only, at each element of the phased array. For ease of implementation, phase-only perturbations are usually desired and provide acceptable null depths. However, the phase shift at each array element will vary with the frequency of the transmitted signal. As a result, the depth and pointing accuracy of the transmit null will not be uniform over the bandwidth of the transmitted signal. A more robust transmit nulling approach is to insert a tapped delay line (TDL) behind each array element instead of a phase shift. As shown in this paper, the null depths achieved over wide signal bandwidths are far superior to conventional phase-only approaches.**

I. Problem Description

An important capability in modern phased array systems is the ability to place nulls in the antenna transmit pattern. Transmit nulls are useful for mitigating interference in dense operating environments and for reducing the unwanted backscatter from clutter. In most practical systems, amplitude and phase control is not available at the array element level. Instead, independent phase commands are applied at each array element to form the desired spatial null, with the amplitude weight at each element fixed to unity. Some common computational techniques for computing transmit nulls are described in [1] – [4].

Typically, the phase weights to be applied at each element are computed for the center frequency of the array, which corresponds to half-wavelength spacing between array elements. Furthermore, the phase shifter behind each element is calibrated for the array center frequency. As a result, for frequencies in the transmitted signal bandwidth other than the array center frequency, the phase shift at each array element will deviate from the desired value, causing the transmit null to change pointing direction.

To illustrate the impact of signal bandwidth on transmit nulls, consider Figure 1 which shows a phase-only null computed using Smith's algorithm for a uniform linear array with 32 elements [4]. The plot shows a deep null at precisely the desired direction, which is 19.57° azimuth. Because an ideal array is assumed with no random noise or errors present, the null depth is essentially infinite.

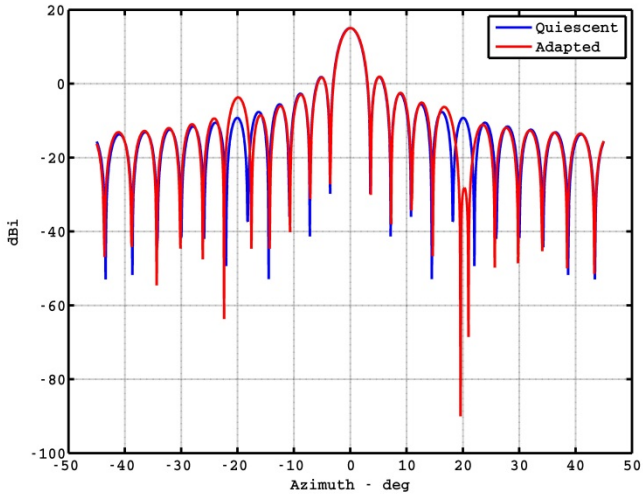

Figure 1. Phase-Only Transmit Null Computed at Array Center Frequency; Quiescent vs Adapted Pattern

In reality, this null is a function of frequency, as seen in the frequency-dependent array pattern of Figure 2. The null is indicated by the nearly vertical yellow line at 19.57°. Upon close examination, it is clear that this line is not exactly vertical. Instead, the line corresponding to the null exhibits a frequency-dependent slope, which indicates that the direction of the null is a function of frequency. In fact, Figure 3 clearly illustrates the shift in null direction for different signal frequencies, as shown by frequency cuts of the array principal plane pattern.

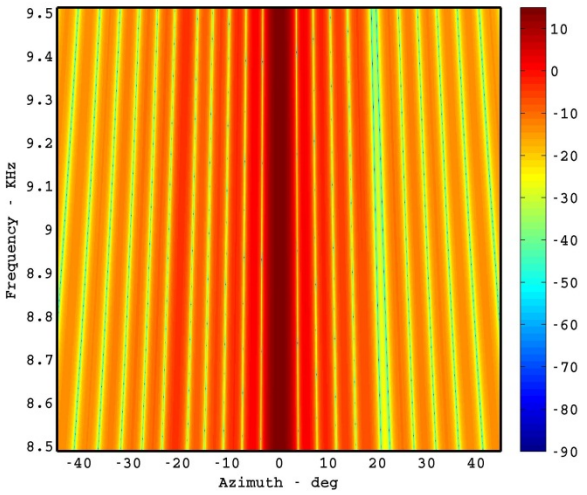

Figure 2. Array Transmit Pattern as a Function of Frequency

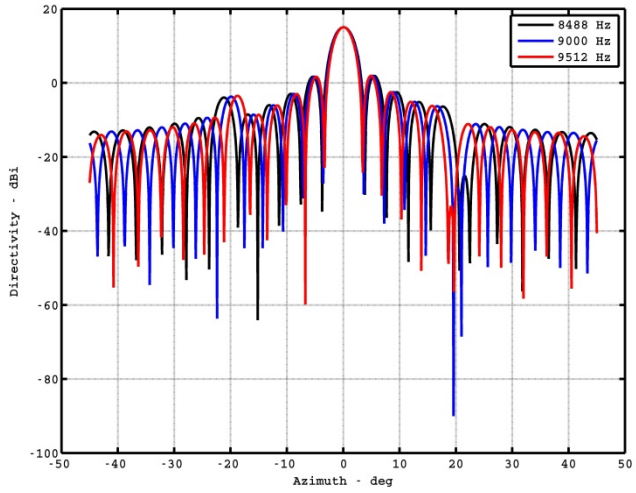

Figure 3. Frequency Cuts of Array Transmit Pattern

II. TAPPED DELAY LINE ARCHITECTURE FOR WIDEBAND NULLS

A. *Tapped Delay Line Architecture*

Figure 4 illustrates the proposed array architecture for forming wideband transmit nulls. This array architecture has been previously described in the literature for other wideband beamforming applications [5, 6]. Behind each array element is a Tapped Delay Line (TDL) with J real taps spaced T_s seconds apart. This architecture can form N nulls at $J/2$ frequencies.

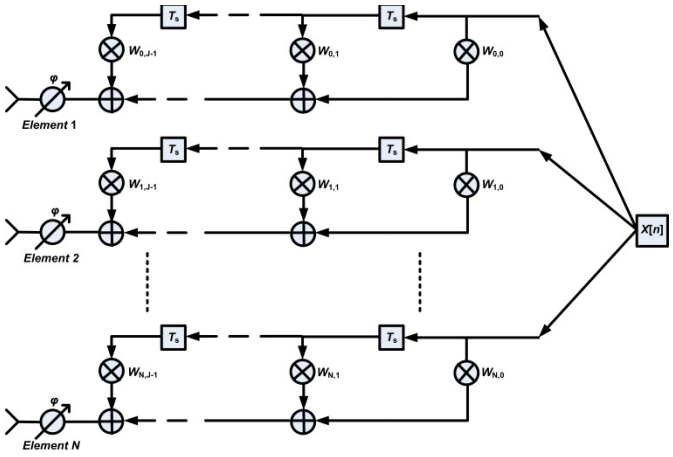

Figure 4. Wideband Array Architecture

The impulse response of a TDL array with N elements can be written as

$$H(\omega,\theta)=\sum_{m=0}^{J-1}e^{-jm\omega T_s}\sum_{n=0}^{N-1}w_{nm}e^{-jn\varphi} \tag{1}$$

where w_{nm} is the mth tap coefficient of the nth array element, and φ is the phase difference between adjacent array elements given by

$$\varphi=\frac{2\pi D\sin\theta}{\lambda}. \tag{2}$$

The parameter D is equal to the distance between array elements, λ is the wavelength of the transmitted signal, and θ is the main beam steering direction with respect to array normal. If the highest transmit frequency of interest is f_1, then D is chosen to be $\lambda_1/2$ to avoid spatial aliasing and T_s is chosen to be $1/(2f_1)$ to avoid temporal aliasing.

B. *Objective Function*

To compute the TDL coefficients for a wideband null, the Signal-to-Noise-plus-Interference Ratio (SINR) integrated over the signal bandwidth of interest for a hypothetical interference source in the direction of the desired null is maximized. This objective function is derived as follows.

Define a frequency dependent steering vector for a linear array with N elements in the direction θ as

$$\mathbf{v}(\theta,f)=[v_1(\theta,f),v_2(\theta,f),\ldots,v_N(\theta,f)]^{\mathbf{T}}, \tag{3}$$

where each component in (3) is given by

$$v_k(\theta,f)=\exp\left(j2\pi D\tfrac{f}{c}\sin\theta(k-1)\right),\qquad k=1,\ldots,N \tag{4}$$

with D equal to the interelement spacing, f the transmit signal frequency, θ the steering angle of the signal with respect to array normal, and c the speed of light.

A vector $\mathbf{w}$ of frequency-dependent weights to be applied to each array element is defined as

$$\mathbf{w}(f) = [w_1(f), w_2(f), \ldots, w_N(f)]^{\mathrm{T}} \tag{5}$$

where $w_j(f)$ is the frequency response of the jth TDL $h_j[n]$ and

$$w_j(f) = H_j(f) = \sum_{k=0}^{J-1} h_j[k] e^{-j\omega T_s k} . \tag{6}$$

The frequency-dependent signal $\mathbf{R}_{vv}$ and noise $\mathbf{N}_{vv}$ covariance matrices can be written for the main beam steering direction θ and the direction θ_1 of the desired null as

$$\mathbf{R}_{vv}(f) = \mathbf{v}(\theta, f)\mathbf{v}(\theta, f)^H , \tag{7}$$

$$\mathbf{N}_{vv}(f) = \beta \mathbf{v}(\theta_1, f)\mathbf{v}(\theta_1, f)^H + \sigma^2 \mathbf{I} \tag{8}$$

where σ^2 is the power of a zero-mean additive white noise Gaussian process, and β is a real positive scalar. The cost function to be maximized over the signal bandwidth of interest is the integrated SINR defined as

$$\xi = \int_{f_0}^{f_1} \frac{\mathbf{w}^H \mathbf{R}_{vv} \mathbf{w}}{\mathbf{w}^H \mathbf{N}_{vv} \mathbf{w}} W(f) df , \tag{9}$$

where f_0 and f_1 are the frequency endpoints of the signal bandwidth and $W(f)$ is a scalar nonnegative real weighting function. The metric used to gauge nulling performance is the average null depth d over the bandwidth of interest, defined as

$$d = \frac{1}{P} \sum_{k=0}^{P-1} \left| G(f_k, \theta_1) \right|^2 , \tag{10}$$

where P is the number of frequency samples within the signal bandwidth and $G(f, \theta)$ is the frequency-dependent array voltage pattern. For the case where M_n nulls in the array pattern are desired, the noise covariance matrix is written as

$$\mathbf{N}_{vv}(f) = \beta \sum_{j=1}^{M_n} \mathbf{v}(\theta_j, f)\mathbf{v}(\theta_j, f)^H + \sigma^2 \mathbf{I} . \tag{11}$$

C. Gradient Computation

To maximize the integrated SINR ξ, the conjugate gradient algorithm may be used. This algorithm requires computing the gradient of ξ with respect to the TDL coefficients. Define the matrix $\mathbf{W}$ of TDL coefficients for N array elements with J taps each, and the delay chain vector $\mathbf{e}(f)$ as follows

$$\mathbf{W} = \begin{bmatrix} h_0[0] & h_0[1] & \cdots & h_0[J-1] \\ h_1[0] & h_1[1] & \cdots & h_1[J-1] \\ \vdots & \vdots & \ddots & \vdots \\ h_{N-1}[0] & h_{N-1}[1] & \cdots & h_{N-1}[J-1] \end{bmatrix}, \tag{12}$$

and

$$\mathbf{e}(f) = \begin{bmatrix} 1 & e^{-j2\pi f T_s} & \cdots & e^{-j2\pi f T_s (J-1)} \end{bmatrix}^{\mathrm{T}} . \tag{13}$$

Then

$$\mathbf{w}(f) = \mathbf{W}\mathbf{e}(f) . \tag{14}$$

The gradient of ξ with respect to $\mathbf{W}$ can be computed by taking the partial derivatives of ξ with respect to $h_k[j]$ (denoted h_{kj}) as follows

$$\nabla \xi_{kj} = \frac{\partial}{\partial h_{kj}} \int_{f_0}^{f_1} \frac{\mathbf{w}^H(f)\mathbf{R}_{vv}(f)\mathbf{w}(f)}{\mathbf{w}^H(f)\mathbf{N}_{vv}(f)\mathbf{w}(f)} W(f) df , \tag{15}$$

with $0 \le j \le J-1$ and $0 \le k \le N-1$. For simplicity, assume $W(f) = 1$. By the Dominated Convergence Theorem [7], the partial derivative may be brought inside the integral to yield

$$\nabla \xi_{kj} = \int_{f_0}^{f_1} \frac{\partial}{\partial h_{kj}} \frac{\mathbf{w}^H \mathbf{R}_{vv} \mathbf{w}}{\mathbf{w}^H \mathbf{N}_{vv} \mathbf{w}} df = \int_{f_0}^{f_1} \frac{\partial}{\partial h_{kj}} \frac{\mathbf{e}^H \mathbf{W}^H \mathbf{R}_{vv} \mathbf{W}\mathbf{e}}{\mathbf{e}^H \mathbf{W}^H \mathbf{N}_{vv} \mathbf{W}\mathbf{e}} df , \tag{16}$$

where the frequency argument f has been suppressed.

Useful relations for a matrix $\mathbf{X}$ and vectors $\mathbf{a}$ and $\mathbf{b}$ are

$$\frac{\partial}{\partial \mathbf{X}} \mathbf{a}^H \mathbf{X} \mathbf{b} = \bar{\mathbf{a}} \mathbf{b}^T , \quad \frac{\partial}{\partial \mathbf{X}} \mathbf{a}^H \mathbf{X}^H \mathbf{b} = \mathbf{b} \mathbf{a}^H , \tag{17}$$

where the overbar denotes complex conjugation. Using these relations and the fact that the matrices $\mathbf{R}_{vv}$ and $\mathbf{N}_{vv}$ are Hermitian yields the derivatives

$$\begin{aligned} \frac{\partial}{\partial \mathbf{W}} \mathbf{e}^H \mathbf{W}^H \mathbf{R}_{vv} \mathbf{W}\mathbf{e} &= 2\,\mathrm{Re}\{\mathbf{R}_{vv} \mathbf{W}\mathbf{e}\mathbf{e}^H\}, \\ \frac{\partial}{\partial \mathbf{W}} \mathbf{e}^H \mathbf{W}^H \mathbf{N}_{vv} \mathbf{W}\mathbf{e} &= 2\,\mathrm{Re}\{\mathbf{N}_{vv} \mathbf{W}\mathbf{e}\mathbf{e}^H\}. \end{aligned} \tag{18}$$

Next using the quotient rule yields

$$\nabla \xi_{\mathbf{W}} = \int_{f_0}^{f_1} \frac{\boldsymbol{\Gamma}(f)}{\delta(f)} df , \tag{19}$$

where

$$\Gamma(f) = \left(\mathbf{e}^H \mathbf{W}^H \mathbf{N}_{vv} \mathbf{W} \mathbf{e}\right)\left(2\,\mathrm{Re}\left\{\mathbf{R}_{vv} \mathbf{W} \mathbf{e} \mathbf{e}^H\right\}\right) - \left(\mathbf{e}^H \mathbf{W}^H \mathbf{R}_{vv} \mathbf{W} \mathbf{e}\right)\left(2\,\mathrm{Re}\left\{\mathbf{N}_{vv} \mathbf{W} \mathbf{e} \mathbf{e}^H\right\}\right), \quad (20)$$

and

$$\delta(f) = \left(\mathbf{e}^H \mathbf{W}^H \mathbf{N}_{vv} \mathbf{W} \mathbf{e}\right)^2. \quad (21)$$

D. Conjugate Gradient Algorithm

The stated optimization objective is to maximize the integrated SINR over all **W**. Equivalently, the integrated Noise-plus-Interference-to-Signal ratio (reciprocal of the SINR) may be minimized over all **W**. The pseudocode for implementing this unconstrained minimization program using the conjugate gradient algorithm is presented next.

1. Set the initial TDL coefficients $\mathbf{W}_0$. A possible initial condition for each TDL is an arbitrary Type-1 finite impulse response (FIR) filter with linear phase.
2. Let $\mathbf{h}_0 = -\nabla\xi_{\mathbf{W}}(\mathbf{W}_0)$.
3. Let $\mathbf{g}_0 = \mathbf{h}_0$.
4. For each iteration j = 0, 1,… compute a step size λ_j using any line optimization routine. Alternatively, set λ_j to a small value that ensures convergence.
5. Set $\mathbf{W}_{j+1} = \mathbf{W}_j + \lambda_j \mathbf{h}_j$.
6. Set $\mathbf{g}_{j+1} = -\nabla\xi_{\mathbf{W}}(\mathbf{W}_{j+1})$.
7. Set $\mu_j = \dfrac{(\mathbf{g}_{j+1} - \mathbf{g}_j)^{\mathrm{T}} \mathbf{g}_{j+1}}{\|\mathbf{g}_j\|^2}$.
8. Set $\mathbf{h}_{j+1} = \mathbf{g}_{j+1} + \mu_j \mathbf{h}_j$.
9. Increment j and go to Step 4.

The chosen objective function will in general have many local minima. The final solution therefore will depend to some degree on the initial condition chosen for the algorithm. A suitable initial condition for **W** which yields reasonable results is to set the TDL for each array element equal to an arbitrary Type-1 FIR filter. Figure 5 displays the evolution of the conjugate gradient algorithm. The figure shows that SINR increases rapidly until it approaches a stationary point where the gradient tends towards zero.

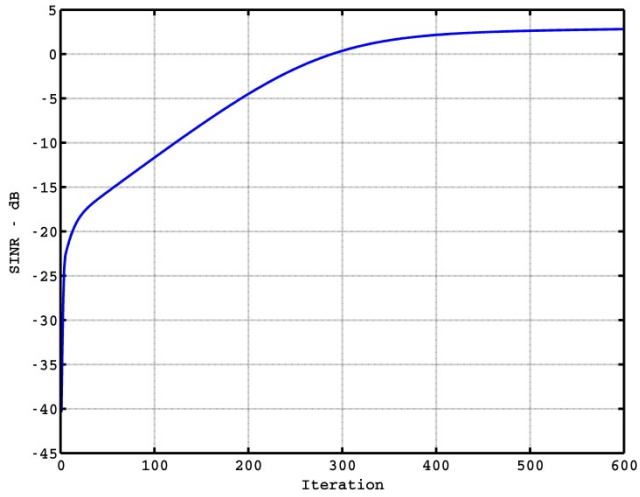

Figure 5. SINR vs Iteration

E. Simulated Results

Figure 6 illustrates an optimized array pattern with a point null created at 19.57° azimuth for a linear array of 32 elements over a fractional bandwidth of 40%. Each TDL has 3 real taps. In this example, the main beam is steered broadside to 0°, as indicated by the dark red vertical region. Figure 7 shows three frequency cuts of the array pattern in Figure 6. The average depth of the null over the signal bandwidth is −88.7 dBi. Figure 8 is a close-up view of the point null at 19.57°. Figure 9 plots the null depth at 19.57° as a function of frequency. This plot shows a deep null over the entire signal bandwidth.

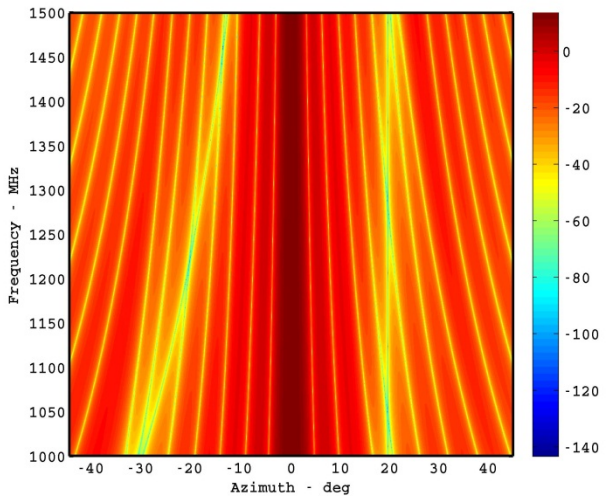

Figure 6. Array Pattern – Point Null Solution

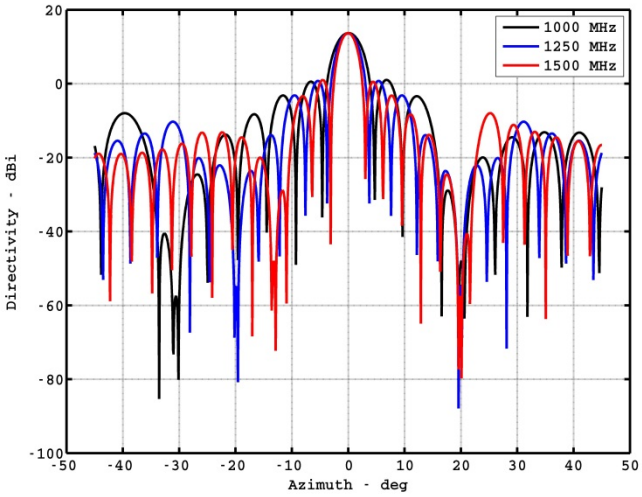

Figure 7. Array Pattern Frequency Cuts – Point Null Solution

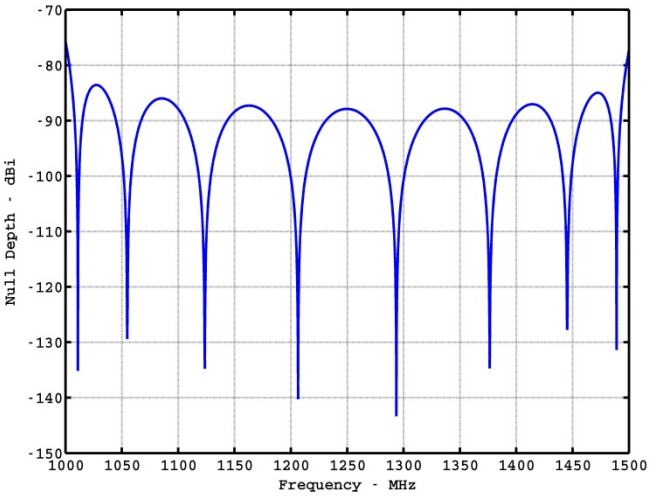

Figure 9. Null Depth vs Frequency – Point Null Solution

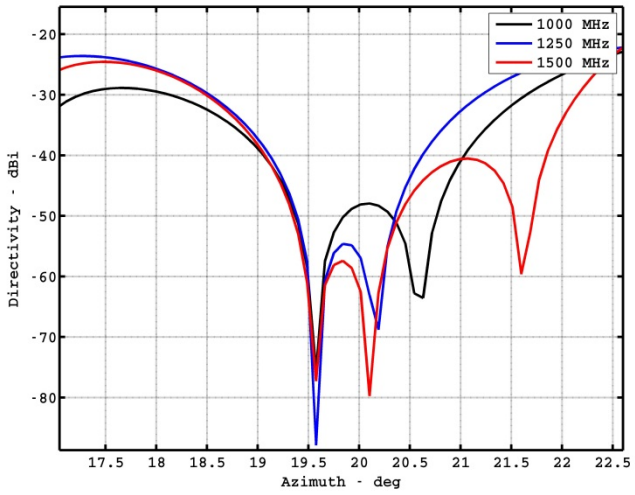

Figure 8. Principal Plane Cuts of Point Null Solution – Close-Up View

A wider transmit notch can be created by placing several point nulls together in close sequence. Figures 10 and 11 show the array pattern for a 4° transmit notch created using 5 point nulls spaced 1° apart between 19.57° and 23.53°. The fractional bandwidth of the transmit signal is still 40%. The average depth of the null over the signal bandwidth is −94.7 dBi. Each TDL consists of 3 real taps. Figure 12 provides a close-up view of the transmit notch for different frequencies, and Figure 13 illustrates the null depth as a function of frequency. Both plots show a deep null over almost the entire signal bandwidth, except towards the band edges where the null degrades.

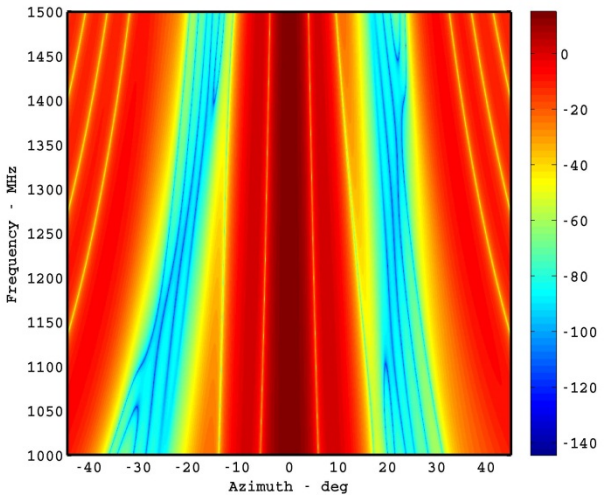

Figure 10. Array Pattern – Transmit Notch Solution

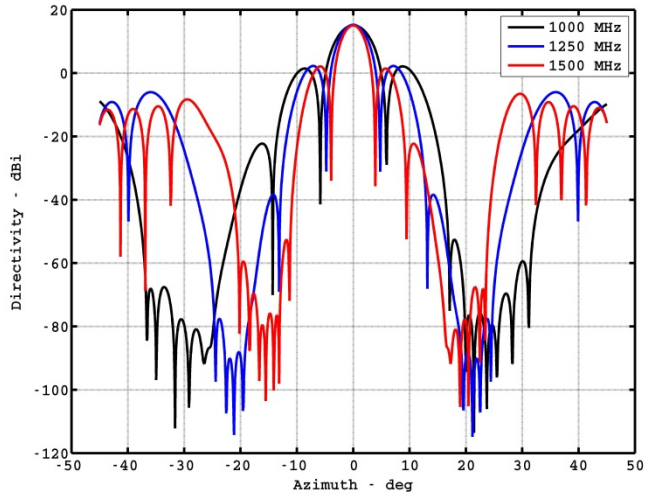

Figure 11. Array Pattern Frequency Cuts (1, 1.25, 1.5 GHz); Transmit Notch Solution

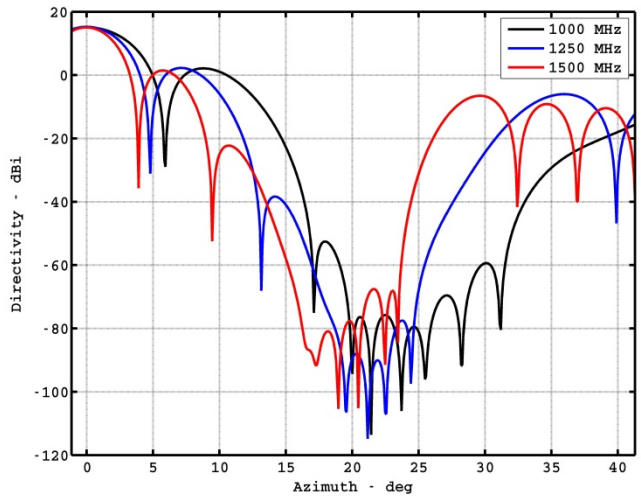

Figure 12. Transmit Notch – Close-Up View

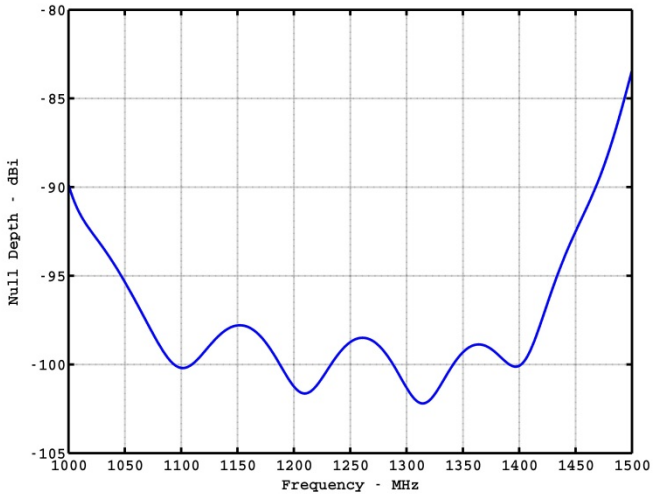

Figure 13. Null Depth vs Frequency – Transmit Notch

III. TRANSMIT SIGNAL DISTORTION

The placement of TDLs behind each array element is excellent for forming wideband nulls as the previous results show. However, the frequency response of each TDL will modify the spectrum of the transmit signal at each array element. The coherent sum in space of the distorted transmit signal from each array element may then result in an erroneous main beam signal. Moreover, because the TDL coefficients will be different for every combination of null location and main beam steering direction, the distortion induced in the main beam signal may be unpredictable.

Consider the TDL coefficients shown in Figure 14 for the transmit notch example. The impulse response of the TDL at any one array element can be determined by fixing the array element index along the x-axis and looking vertically to see the TDL coefficient at each tap delay. This figure shows that the TDLs exhibit an almost even symmetry about the center tap. Therefore one would expect that the TDLs possess a nearly linear phase response. Figures 15 and 16 display the magnitude and phase responses of all the TDLs. As is evident, the phase responses are not exactly linear and the magnitude responses are not exactly flat. Therefore, the original transmit signal will be slightly distorted at the output of each TDL before being radiated into space.

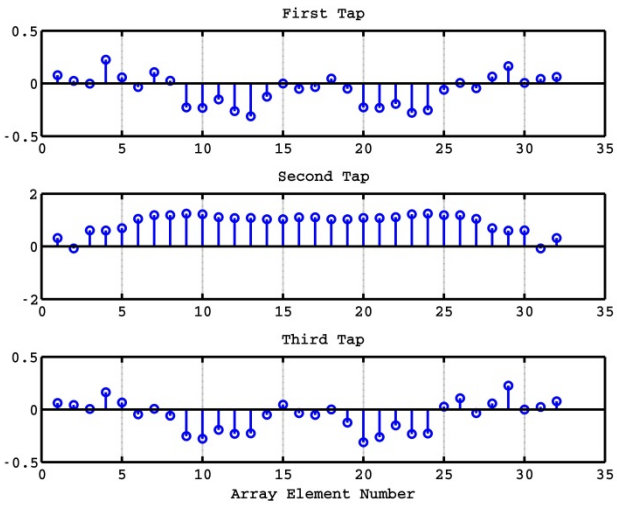

Figure 14. TDL Coefficients – Transmit Notch

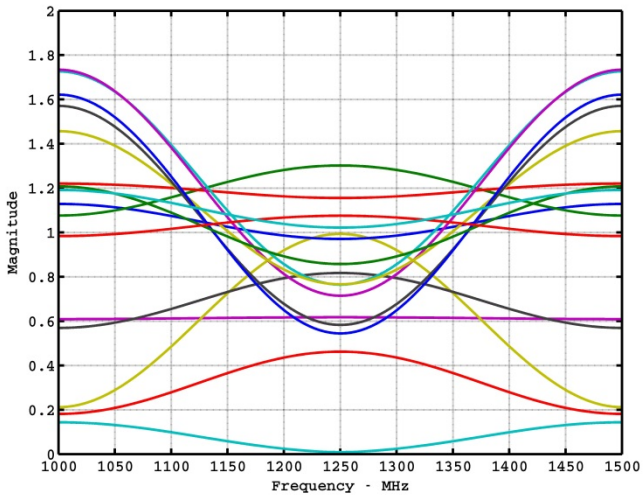

Figure 15. Magnitude Responses of All TDLs – Transmit Notch Solution

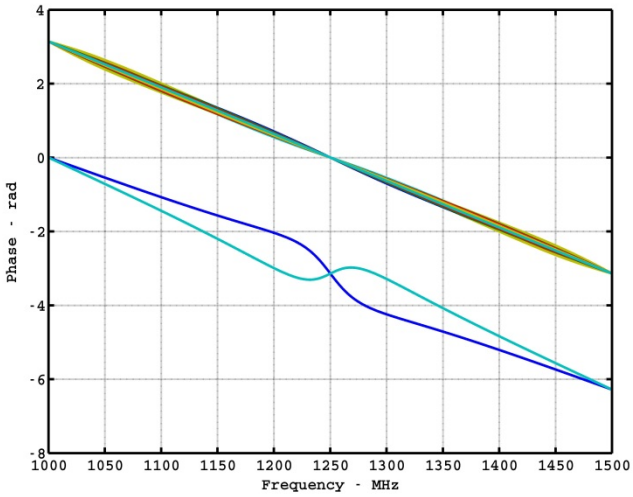

Figure 16. Phase Responses of All TDLs – Transmit Notch Solution

The signal distortion induced in the spectrum of the transmit signal is illustrated in Figure 17. The assumed transmit signal in this case is not any specific radar waveform, but rather a more general autoregressive spectrum. The red curve represents the signal transmitted by the antenna's main beam and the blue curve represents the signal at the input to each TDL. In this case, the distortion induced by the TDL architecture in the magnitude spectrum of the transmit signal is very benign.

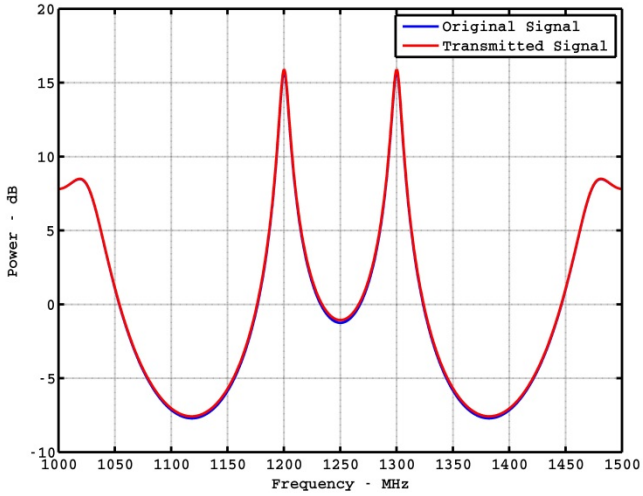

Figure 17. Transmit Signal Distortion – Transmit Notch

For the transmit notch example, the frequency response of the array in the main beam steering direction is shown in Figure 18. This curve can be computed by holding the azimuth angle θ fixed in (1) and (2). The deviation in mainbeam directivity as a function of frequency is seen to be only approximately 0.2 dB.

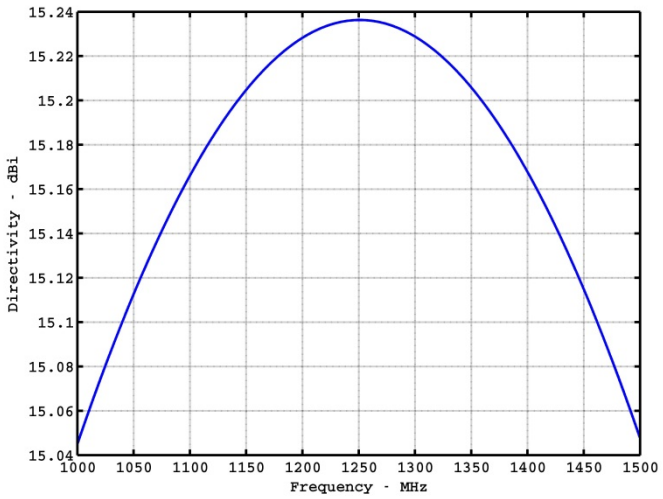

Figure 18. Array Response in Main Beam Direction – Transmit Notch

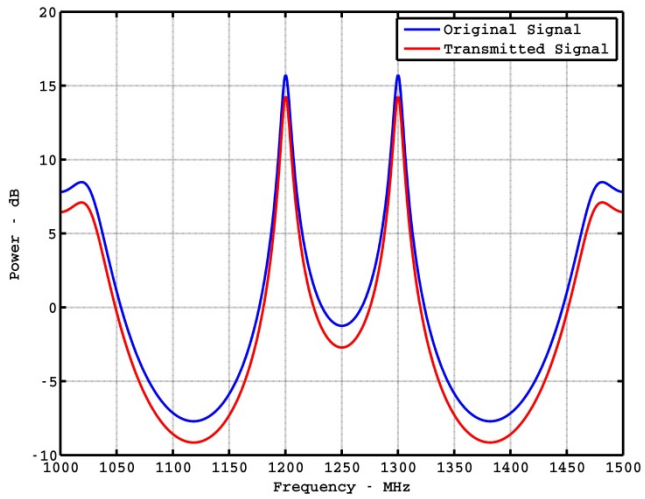

Figure 19. Transmit Signal Distortion – Point Null Solution

However, since every TDL solution will be different for all various transmit nulls, there is no reason to expect benign signal distortion on every occasion. Indeed, Figure 19 illustrates the signal distortion induced by the point null solution shown earlier in Figures 6 and 7. In this case, the distortion created in the mainbeam signal is more pronounced. Thus, for particular TDL solutions, the improved bandwidth performance of the transmit null may induce undesirable errors in the mainbeam transmit signal.

IV. CONCLUSIONS

This paper explored the performance of a wideband array architecture with tapped delay lines placed behind each array element to create transmit nulls in space over wide signal bandwidths. An objective function to be maximized was defined based on the SINR for a hypothetical interference source at the null location, and an algorithm was presented to find a solution. Simulated results show deep nulls in the array transmit pattern over large fractional bandwidths. For certain TDL solutions, it is possible that the mainbeam signal spectrum will be appreciably distorted. This drawback will be the subject of future research.

REFERENCES

[1] D. Day, "Robust Phase-Only Nulling for Adaptive and Non-Adaptive Phased Arrays," *Proceedings 2007 Asilomar Conference on Signal, Systems and Computers*, Monterey, CA., November 4-7, 2007.

[2] E. Dufort, "Pattern Synthesis Based on Adaptive Array Theory," *IEEE Transactions on Antennas and Propagation*, Vol. 37, No. 8, August 1989.

[3] H. Steyskal, "Simple Method for Pattern Nulling by Phase Perturbation," *IEEE Transactions on Antennas and Propagation*, Vol. 31, No. 1, January 1983.

[4] S. T. Smith, "Optimum Phase-only Adaptive Nulling," *IEEE Transactions on Signal Processing*, Vol. 47, No. 7, July 1999.

[5] N. Ishii and R. Kohno, "Spatial and Temporal Equalization Based on an Adaptive Tapped Delay Line Array Antenna," *Proceedings 5th IEEE International Symposium on Wireless Networks; Catching the Mobile Future*, The Hague, The Netherlands, September 18-23, 1994.

[6] Y. Zhao, W. Liu, and R. Langley, "Subband Design of Fixed Wideband Beamformers Based on the Least Squares Approach," *Elsevier Journal on Signal Processing*, Vol. 91, September 2010.

[7] G. B. Folland, *Real Analysis; Modern Techniques and Their Applications*, 2nd ed., Wiley Interscience, Hoboken, NJ, 1999.